

# Significant association between the skewed natural antibody repertoire of *Xid* mice and resistance to *Trypanosoma cruzi* infection

Eduardo-César Santos-Lima<sup>1</sup>, Rita Vasconcellos<sup>1</sup>, Bernardo Reina-San-Martín<sup>1</sup>, Constantin Fesel<sup>2</sup>, Anabela Cordeiro-da-Silva<sup>1</sup>, Armand Berneman<sup>2</sup>, Alain Cosson<sup>1</sup>, Antonio Coutinho<sup>2</sup> and Paola Minoprio<sup>1</sup>

<sup>1</sup> Département d'Immunologie, Institut Pasteur, Paris, France

<sup>2</sup> Instituto Gulbenkian de Ciência, Oeiras, Portugal

The *Xid* mutation predominantly affects the development of B cells and consequently the levels and composition of natural antibodies in sera. In contrast to the congenic and susceptible BALB/c strain, immunodeficient BALB.*Xid* mice display a resistant phenotype both to acute *Trypanosoma cruzi* infection and to the development of severe cardiopathy. Because natural antibodies are known to be basically self-antigen driven, IgM and IgG natural antibody repertoires (NAR) were compared before and during infection in these two strains. The analysis revealed fundamental alterations of IgM and IgG NAR in pre- and post-infected *Xid* mice. In particular, relatively increased natural (pre-existing) autoreactive IgG, dominated by the unique recognition of a single band in autologous heart extracts, was typical for uninfected *Xid* mice. This natural autoreactive IgG directed to heart antigens disappeared early after infection not only in *Xid*, but also in individual BALB/c mice that survived the acute infection. Conversely, the subgroup of BALB/c mice that died early after infection presented the most pronounced instances of the rapid, relative increase of IgM reactivities to self and non-self proteins. These results suggest that self-reactive NAR may play a role in an immunoregulatory mechanism relevant for the determination of susceptibility/resistance to infections. This may act either by influencing specific responses, or by modulating the self-aggressive components responsible for pathology.

**Key words:** B cell repertoire / *Xid* / Natural antibody / *Trypanosoma cruzi*

Received	20/1/00
Revised	9/11/00
Accepted	20/11/00

## 1 Introduction

Chagas' disease, caused by the parasitic protozoan *Trypanosoma cruzi* evolves through a chronic pathology of heart and digestive tract muscle, with intense lymphocyte infiltration and consequent heart failure or megasyndromes [1]. *T. cruzi* infection induces an intense polyclonal activation of all lymphocyte classes, with hypergammaglobulinemia and general immunosuppression of responses towards unrelated antigens [2, 3]. Several reports suggest that chronic-phase pathology results from autoimmune mechanisms, which in turn may be triggered by the polyclonal lymphocyte activation char-

acteristic of acute infection [1, 2, 4, 5], although a direct causality has, as yet, not been established [6, 7]. Molecular mimicry of various host molecules by parasite antigens has been shown [8, 9]. Nevertheless, such a putative relationship of acute infection to chronic autoimmunity could also result from the disruption of regulatory mechanisms and/or general alterations of repertoire expression, rather than from the activation of single autoreactive clones [10].

In contrast to most mouse strains that die of the acute *T. cruzi* infection, BALB.*Xid* (*Xid*, X-linked immunodeficient) mice survive infection, present a limited polyclonal lymphocyte activation and enter a life-long chronic phase with reduced tissue cardiopathy [11]. We have previously shown that the natural resistance of *Xid* mice to *T. cruzi* infection could be due, at least in part, to an elevated production of IFN- $\gamma$ , caused by a relative deficiency in IL-10 [12]. Indeed, the central role of IFN- $\gamma$  in the control of infection was supported by the reestablishment of susceptibility of *Xid* mice by *in vivo* treatment with anti-IFN- $\gamma$

[1 20519]

The first two authors contributed equally to this publication.

**Abbreviations:** **NAR:** Natural antibody repertoires **NAb:** Natural antibody **BA:** BALB/c mouse **Xid:** X-linked immunodeficient mouse **PCA:** Principal component analysis

antibodies, and by natural (adoptive fostering) or experimentally (antibody treatment) induced deletion of IFN- $\gamma$ -producing V $\beta$ 6-bearing T cells [12, 13]. High levels of IFN- $\gamma$  observed in resistant *Xid* mice may also result from alterations in the levels of microbial colonization consecutive to their immunodeficiency. In fact, *Xid* mice carry a point mutation in the pleckstrin homology domain of the Bruton's tyrosine kinase (Btk) gene [14], resulting in severe B cell defects such as a reduced level of conventional B2 cells (IgM<sup>+</sup>IgD<sup>+</sup>CD5<sup>-</sup>), absence of B-1 cells (IgM<sup>+</sup>IgD<sup>o</sup>CD5<sup>+</sup>), low levels of IgM and IgG3 immunoglobulins, signaling defects in response to BCR stimulation and CD38 as well as very poor responses to T cell-independent antigens [15–19]. B-1 cells have been shown to play an essential role in establishing the fetal and adult natural antibody repertoires (NAR), and to contribute importantly to the production of self-reactive natural antibodies (NAb) [20, 21]. It is of interest that this cell subpopulation (absent in *Xid* mice) is preferentially expanded during *T. cruzi* infection in susceptible mouse strains [22].

The association of the *Xid* immunodeficiency with resistance to *T. cruzi* infection may seem paradoxical, but it has also been recorded in *Leishmania major*, *Staphylococcus aureus*, and MAIDS virus infections [23–25]. Regardless of the primary alterations leading to the resistance of *Xid* mice, but given the important role of self-reactive NAb in infections [26, 27], putative deviations in NAR in *Xid* mice could also be associated to their unusual resistance to these infections. An unequal isotype distribution of specific and nonspecific antibodies appearing after *T. cruzi* infection of wild-type and *Xid* mice has been described [11, 28]. We addressed the above hypothesis by comparing the relative contribution of NAR components to each class of immunoglobulins in naive and *T. cruzi*-infected *Xid* and BALB/c wild-type (BA) mice, using a Western blot technique that allows the semiquantitative scoring of serum reactivities towards a very large panel of extracts of autologous (self) or heterologous antigens [29–34]. Serum IgM and IgG reactivities were assayed on extracts of syngeneic tissues, bacteria and *T. cruzi*, after standardizing the total IgM and IgG concentrations of all sera to 10  $\mu$ g/ml for IgM and 100  $\mu$ g/ml for IgG. In this way, we generally scored serum reactivities in relation to the total pool of antibodies of the same class of immunoglobulins in the individual serum.

## 2 Results

### 2.1 *Xid* and BA mice markedly differ in their natural (auto) antibody repertoire

Analysis of serum reactivities from uninfected, unmanipulated mice, on antigenic extracts of syngeneic heart and liver, *E. coli* and *T. cruzi* showed that *Xid* and BA mice markedly differ in their NAR (Fig. 1). In terms of absolute concentration, serum from uninfected BA and *Xid* mice contains comparable levels of IgG, in contrast to drastically reduced IgM observed in *Xid* (Fig. 2 and [11, 28]). It is worth noting that to assess IgM repertoires, sera from individual BA mice required greater dilution than sera from *Xid* individuals. Despite this, when serum samples were tested at the same IgM concentration, most IgM reactivities score higher for BA than for *Xid* sera, in both self and heterologous antigens (Fig. 1A.). This indicates that, regardless of the lower IgM serum concentrations, *Xid* sera embodied IgM repertoires that are relatively less reactive to conventional antigens. Thus, when tested on autoantigens (heart and liver), *Xid* serum IgM lacks entire sets of reactivities that are well represented in BA serum IgM, demonstrating that the *Xid* NAR is severely defective in physiological autoreactivity. Interestingly, lower reactivity was similarly scored in *Xid* IgM towards *T. cruzi* antigens that are abundantly recognized by BA NAb. When the scores obtained from the sectorized densitometry towards all antigens were submitted to multivariate analysis (principal component analysis, PCA), these differences appear very clearly, the first resulting principal component readily segregating individual BA and *Xid* mouse strains into non-overlapping areas of the two-dimensional space defined by the first two PCA factors (Fig. 1B).

A similar study of serum IgG NAb of uninfected animals under the same conditions as above revealed another important difference between the two mouse strains. Thus, while natural IgG reactivities to heterologous antigens (*E. coli* and *T. cruzi*, Fig. 1C) are comparable in specificity and intensity between BA and *Xid*, the latter express a richer IgG repertoire towards self, particularly heart, antigens that is reciprocal to their IgM repertoire (Fig. 1A). The scoring of abundant serum IgG autoreactivities of *Xid* in general is exceptional when compared to all other mouse strains analyzed thus far (*i.e.* C57BL/6, BALB/c, DBA/2, *lpr/lpr*; personal unpublished observations and [29–36]).

These results show distinct anti-self NAR of BA and *Xid* mutant mice. On one hand, *Xid* IgM natural antibody reactivities are generally reduced in contrast to those of the *Xid* IgG; on the other hand, IgG NAR of *Xid* is preserved to heterologous antigens, but is clearly more

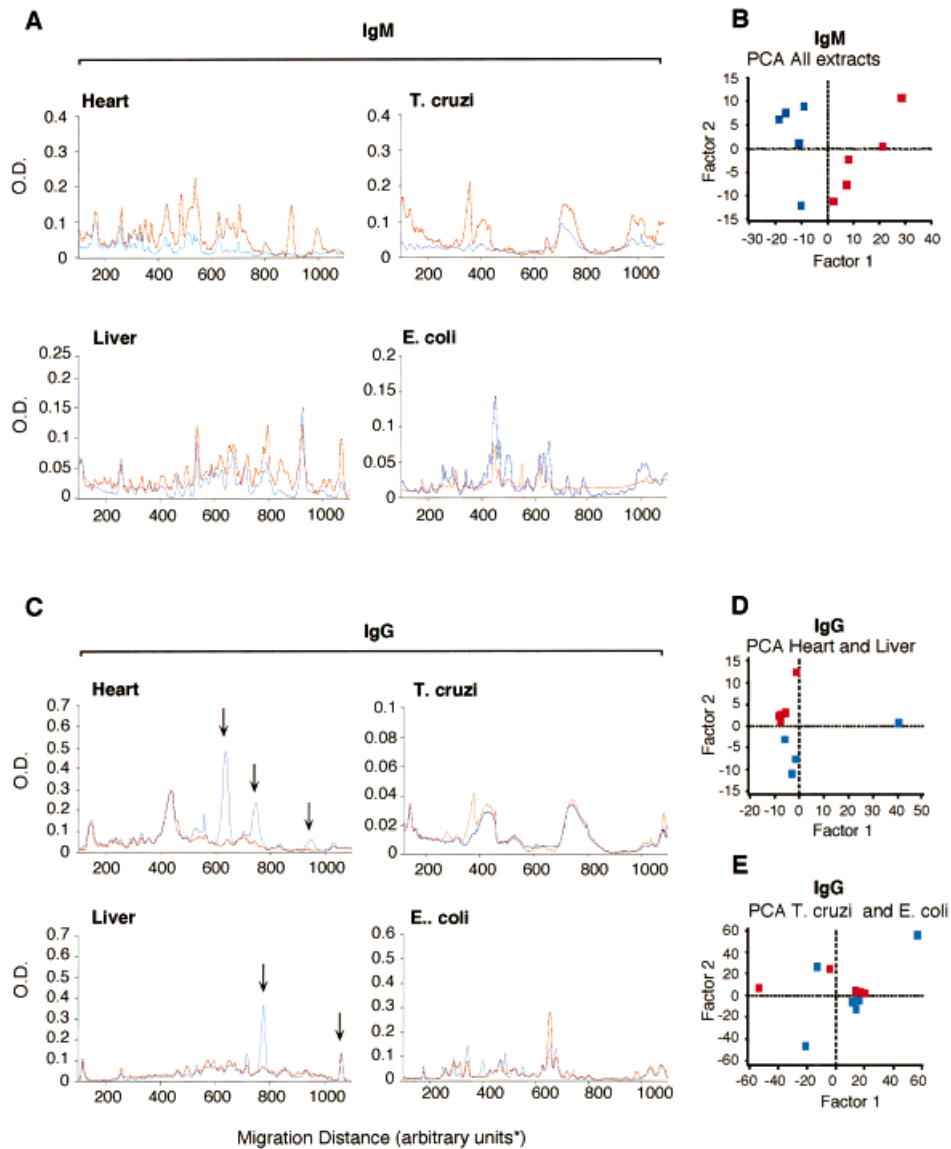


**Fig. 1.** Densitometric profiles and principal components calculated from uninfected BA and *Xid* serum IgM and IgG reactivities to self and non-self extracts. Sera from uninfected mice were tested for IgM or IgG reactivities (after IgM and IgG concentration adjustments to 10  $\mu\text{g/ml}$  and 100  $\mu\text{g/ml}$ , respectively) on blots of autologous liver and heart, as well as on blots of *T. cruzi* and *E. coli* extracts. Average immunoreactivity profiles of five BA and five *Xid* mice on each extract are shown for IgM (A) and for IgG (C). (A) For heart, differences between BA and *Xid* IgM reactivities ( $p=0.01$  for section 26, corresponding to the position 620 on the migration scale). (C) The most pronounced differences between BA and *Xid* IgG reactivities are shown by arrows in heart and liver protein profiles ( $p<0.001$  for section 26, corresponding to the position 620 on the migration scale). Sectorized intensities of IgM reactivities scored on all four extracts analyzed were submitted to PCA. Scores of the resulting first two principal components of the individual BA and *Xid* mice are shown in a two-dimensional plot (B). Sectorized intensities of IgG reactivities scored on heart and liver, as well as *T. cruzi* and *E. coli*, respectively, were submitted to PCA. Scores of the resulting first two principal components of the individual BA and *Xid* mice are shown in two-dimensional plots for self (D) and foreign (E) antigens. BA and *Xid* mice are represented in red or blue lines and squares, respectively.

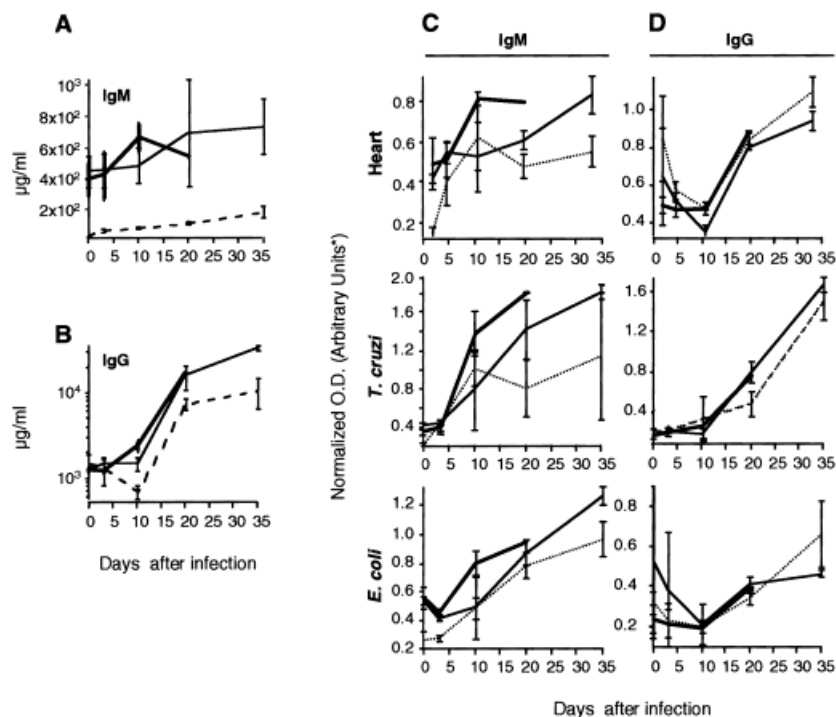


**Fig. 2.** BA and *Xid* total serum IgM and IgG concentrations and reactivities to self and non-self extracts before and throughout the *T. cruzi* infection. Total serum IgM (A, linear scale) and IgG (B, logarithmic scale) concentrations were tested by ELISA and are plotted as a time course. Total IgM (C) and IgG (D) immunoreactivities to autologous heart, *T. cruzi* and *E. coli* extracts were calculated in sera from BA mice dying (thick lines) or surviving (thin lines) the *T. cruzi* infection and *Xid* mice (dashed lines), by scoring the mean normalized absorbance over the entire migration scale and are plotted as a time course. Means and SD for each group are shown for every time point throughout the *T. cruzi* infection.

autoreactive than that of the non-mutant strain. Interestingly, the enhanced *Xid* IgG NAb autoreactivity does not correspond to a nonspecific reinforcement of the entire 'normal' repertoire, but is rather selectively directed to a limited set of autoantigens.

## 2.2 Susceptibility or resistance to *T. cruzi* infection correlates reciprocally with IgM and IgG reactive repertoires throughout infection

Considering that *Btk* mutation leads to a defect of B1 cells, a major source of IL-10 *in vivo*, we investigated whether macrophage effector functions were altered in resistant *Xid* immunodeficient mice. Since IL-10 is a potent down-regulator of IFN- $\gamma$ -mediated and macrophage microbicidal activity, we considered the possibility that *Xid* resistance to infection relies on naturally increased macrophage activity. However, we were able to indirectly exclude this hypothesis by analyzing the state of specific cell activation using the macrophage-induced H<sub>2</sub>O<sub>2</sub> release on stimulation by phorbol myristate acetate. Peritoneal cells obtained from resistant *Xid*

or from susceptible BA mice did not differ significantly before or after infection in their ability to produce H<sub>2</sub>O<sub>2</sub> (Table 1). In fact, it seemed that, after infection, susceptible BA mice present higher increases in macrophage activity following infection than *Xid* mice when compared to uninfected controls. Previous experiments have shown that macrophages obtained from both *Xid* and BA mice exhibit similar low levels of secretion of NO, as measured by NO<sub>2</sub> accumulation in cell supernatants (<1 nM/10<sup>6</sup> cells/ml for both uninfected groups, not shown). These results suggest that the state of macrophage activation in uninfected *Xid* and BA mice could not be *per se* responsible for the differences in susceptibility observed in both models.

We then analyzed alterations in IgM and IgG serum concentrations as well as reactivity patterns in response to *T. cruzi* infection. The dynamics of the total serum concentrations of IgM and IgG showed that susceptibility or resistance to *T. cruzi* infection correlates reciprocally with IgM and IgG reactive repertoires throughout infection (Fig. 2). Absolute IgM concentrations, initially much higher in BA mice, rose slightly in parallel in BA and *Xid*

**Table 1.** Levels of macrophage activation in *Xid* and BA mice

Mice	Infection <sup>a)</sup>	H <sub>2</sub> O <sub>2</sub> release (nmol × 10 <sup>6</sup> cells)
BA	–	<0.01
	+	1.4±0.25
<i>Xid</i>	–	0.6±0.07
	+	1.18±0.18

a) Groups of four mice were infected with 10<sup>4</sup> parasite forms and macrophage activation was quantified at day 15 of infection and compared to uninfected individuals. Results are arithmetic means ± SD.

animals after infection, without evident differences in the kinetics. However, BA mice that died early in acute infection displayed the highest and most rapid increase of IgM up to day 10 (Fig. 2A). Total serum IgG levels in both strains were initially comparable, in spite of known differences in IgG isotype distribution (Fig. 2B, [11]). BA mice that died shortly after infection typically initiated an early (before day 10) increase in their serum IgG levels similar to that observed for the IgM. Interestingly, the IgG levels of two atypical BA mice that survived our observation period of 35 days underwent minor changes, while those of *Xid* mice transiently decreased. Later on in infection, the surviving individuals of both strains displayed a similar tenfold amplification of total IgG serum levels. Although IgG levels in *Xid* mice equally increased, their levels of IgG remained significantly lower throughout infection.

The comparison of relative IgM and IgG reactivities in BA and *Xid* mice to syngeneic heart, *T. cruzi* and *E. coli* extracts throughout the *T. cruzi* infection, keeping constant the Ig concentrations in the immunoblot assay, confirmed that the development of reactivities was clearly different between BA and *Xid* strains (Fig. 2C, D). As already mentioned, uninfected BA mice had a richer IgM NAR than uninfected *Xid* mice. What was surprising, however, was the consistent association of distinct, early repertoire modifications following *T. cruzi* infection with individual susceptibility to the disease within the BA group of mice. In this representative experiment, three typical mice out of five in the BA group that died early after infection presented a clear and relatively higher IgM reactivity to all three (autologous and heterologous) extracts at day 10, parallel to their more pronounced absolute increase in IgM concentration. However, in 'atypical' BA mice that survived acute infection this antibody pool increased slowly during the first 2 weeks of infection, reaching a level comparable to that observed

in the IgM NAR reactivities of resistant *Xid* mice by day 10. In *Xid* mice themselves, which initially presented poor IgM NAR, a slow but significant increase in this pool was seen throughout infection (Fig. 2C).

Interestingly, the relative reactivity of IgG NAR pools to *T. cruzi* extracts was not significantly different between BA and *Xid* mice during parasite infection (Fig. 2D, middle panel). In contrast, dying and surviving mice could be distinguished by their relative reactivities to both heart and *E. coli* extracts during infection. Thus, both *Xid* and the 'atypical' BA mice that survived infection with *T. cruzi* exhibited an early, transient decrease in these IgG reactivities up to day 10 of infection. This early relative decrease of autoreactive (but not *T. cruzi*-specific) IgG coincided in *Xid* with the absolute decrease in total serum IgG (see Fig. 2B), to which it apparently overproportionally contributed. Thereafter, IgG reactivities of 'survivors' and resistant mice increase almost in parallel with those of the susceptible BA mice. The latter show no significant decrease in their IgG reactivities at any point in the infection.

### 2.3 Down-modulated dominant pre-existing heart-specific NAb readily distinguish individuals genetically resistant and susceptible to *T. cruzi* infection

As indicated above, the *Xid* IgG NAR before infection is characterized by a dominant autoreactivity to a certain heart protein (corresponding to a specific molecular mass, see Fig. 1B) hardly recognized in BA mice ( $p < 0.001$ , according to Student's *t*-test). Furthermore, there is an initial general reduction in the extent of heart autoreactivity after *T. cruzi* infection (Fig. 2D). This apparent decrease in autoreactive IgG can also be represented in terms of this dominant specificity scored towards the heart extract. This band, shown in Fig. 3A, dominated the IgG reactivity pattern of uninfected *Xid* mice (position 620 on the migration scale, Fig. 1C, arrowed). Quantitatively, this IgG reactivity in *Xid* mice continuously decreased until day 20 after infection (Fig. 3C). The overall increase in IgM autoreactivity is also reflected in the scores of this section. IgM reactivity scored in this same section was already significantly higher in uninfected BA than in uninfected *Xid* mice (Fig. 3B,  $p = 0.01$ ). Until day 10 following infection, the increase of IgM reactivity observed in all mice was dissimilar within the BA group, which was especially conspicuous and rapid in the typical susceptible BA mice. These findings showed that the down-modulation of dominant pre-existing heart-specific IgG NAb can readily distinguish individuals genetically resistant or susceptible to *T. cruzi* infection.

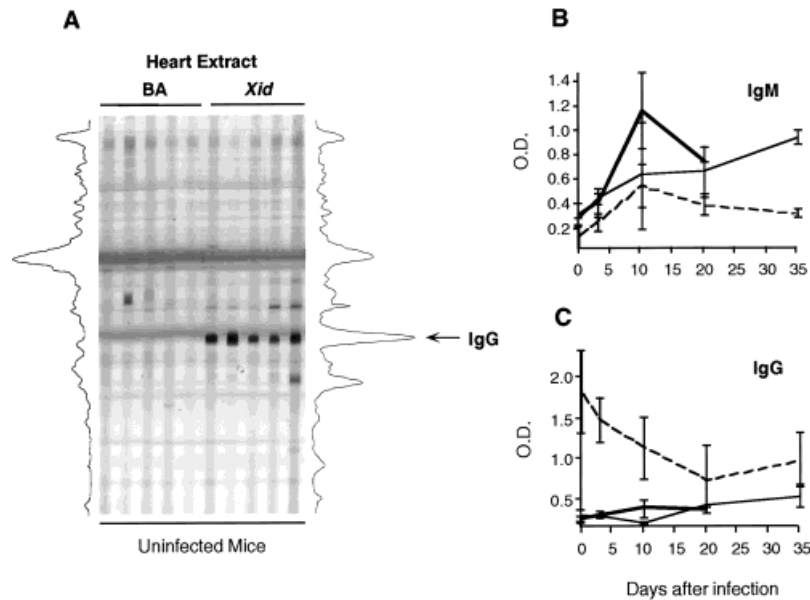


Fig. 3. IgM and IgG reactivity towards a specific band on heart extract before and throughout the *T. cruzi* infection. IgG reactivity to autologous heart extract in sera from uninfected BA and *Xid* mice on immunoblot is shown (A); mean BA (left) and *Xid* IgG profiles (right) are depicted in the sides of the blot. Serum IgM (B) and IgG (C) reactivities at different time points throughout the *T. cruzi* infection were scored as average standardized absorbance in a specific section defined on the migration scale (see position 620 in Fig. 1A and C). Reactivities are plotted as mean and SD inside each group. BA mice, dying (thick lines) or surviving (thin lines) the *T. cruzi* infection and *Xid* mice (dashed lines) are shown.

#### 2.4 BA and *Xid* mice show dissimilar IgM and IgG repertoire structures following *T. cruzi* infection

Our data indicated that the natural pre-existing or early post-infection modifications of IgM/IgG NAR have typical structures that are possibly related to the disease manifestation, and thus may be of prognostic significance in Chagas' disease. Thus, we further performed multivariate statistical analysis attempting to get a representation of these complex IgM and IgG repertoire patterns to determine whether they are dissimilar in BA and *Xid* following *T. cruzi* infection. Quantitations of all section immunoreactivities throughout infection were submitted to PCA, as for the uninfected sera. The following results represent the changes in intrinsic structures of NAR binding patterns of all sera as a result of *T. cruzi* infection. The dynamics for the repertoires throughout infection are shown in Fig. 4 as mean trajectories representing groups of mice, in a two-dimensional display of the first two principal components calculated from all IgM or IgG reactivities scored in the sections previously defined for each extract, respectively. The different time points in each group were connected as trajectories indicating the days before (1) or throughout infection (2–5). All these representations, except for the IgG repertoire to

*E. coli*, (Fig. 4B, bottom) demonstrate clear differences between BA and *Xid* mice. A parallel evolution of repertoire structures, maintaining pre-existing differences during the course of infection, is the major characteristic of the first two PCA factors representing IgM and IgG binding profiles to heart extract, with an initial convergence in the IgG repertoire due to decreasing reactivity in the *Xid* mice (Fig. 4A, B, top panels). Furthermore, the two subgroups of the BA mice, those that survive and those that succumb to infection, can also be discriminated by the trajectories of the IgM reactivity to the heart. The repertoire structure of the survivors changed much less dramatically (Fig. 4A, top). The representations of IgM and IgG binding patterns to *T. cruzi* (middle panels of Fig. 4A, B, respectively) are both characterized by a continuously diverging repertoire structures in the two congenic strains, with relatively little pre-existing differences between BA and *Xid* mice. This divergence in IgM and IgG repertoires began relatively late, from about day 10 after infection. Typical and atypical BA mice were, however, indistinguishable.

Perhaps the most interesting is the representation of IgM binding to *E. coli* extract (Fig. 4A, bottom), which served to further emphasize the distinction between these subgroups of BA mice. A more rapid shift in the vertical com-

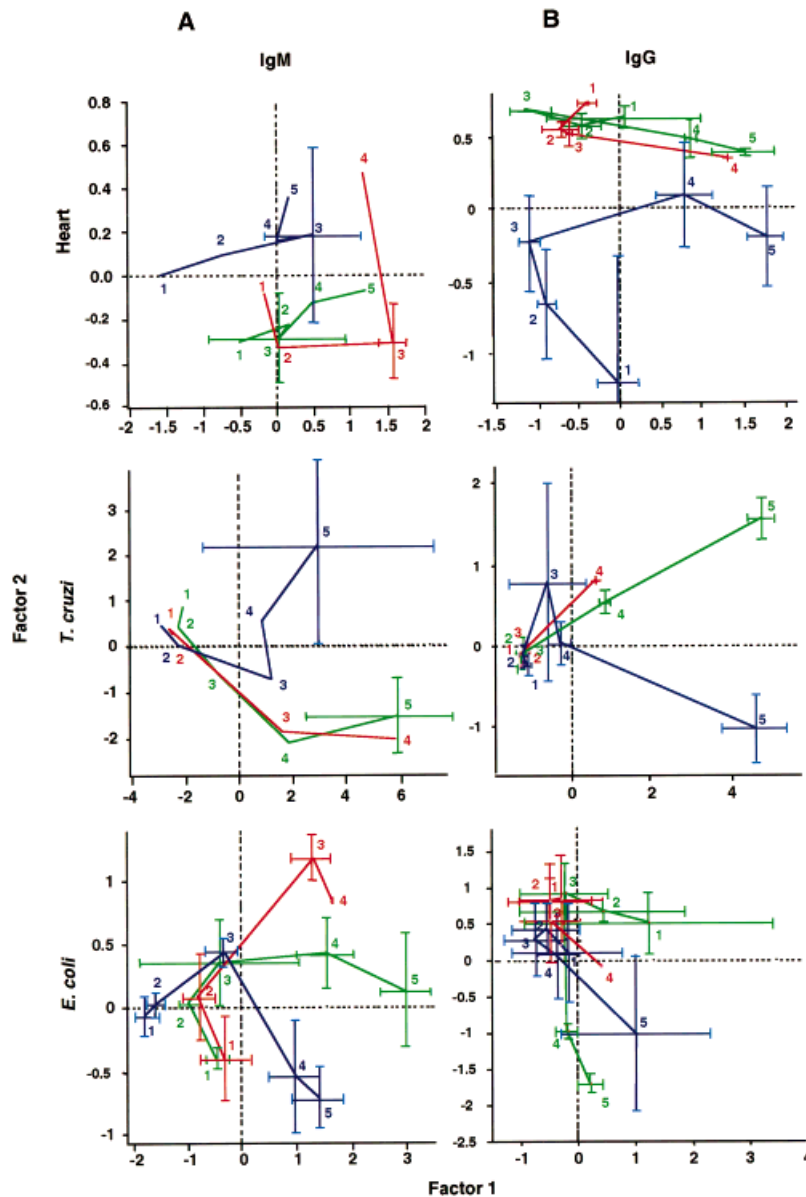


**Fig. 4.** PCA analysis on surviving and dying BA and *Xid* serum IgM and IgG reactivities before and throughout the *T. cruzi* infection. Serum IgM (A) and IgG (B) reactivities scored on immunoblots towards self heart, *T. cruzi* and *E. coli* extracts (in all sections defined on the migration scale) were submitted to separate PCA calculations for every extract and isotype. The two-dimensional plots show average scores and SD of the respective two first principal components for dying (red lines) and surviving (green lines) BA, and *Xid* mice (blue lines), at different time points throughout the infection. The data representing different time points of the three groups of mice were connected to trajectories. Time points (days after infection) are shown as numbers inserted into the trajectories (day 0=1, day 3=2, day 10=3, day 20=4, and day 35=5).

ponent (factor 2) can be seen in the repertoire structures of typical susceptible BA mice, which diverges from the mean trajectory for survivors. This analysis further accentuated the distinction of both subgroups from *Xid* mice, the survivors represented by a trajectory between those for the typically susceptible BA and the resistant *Xid*.

### 3 Discussion

Here we present evidence that the Btk mutation that defines *Xid* results in profound deviations in NAR, and show a differential evolution of serum antibody repertoires in susceptible BALB/c and relatively resistant BALB.*Xid* mice following *T. cruzi* infection. Furthermore, our results suggest that the serum antibody response, as

well as resistance and survival to parasite infection may correlate with the pre-existing NAb pool. *Per se*, these observations open new possibilities for the analysis and prognosis of infectious processes and call attention to the importance of the class regulation of B cell responses.

Following experimental *T. cruzi* infection a high proportion of individuals of conventional mouse strains die early in the acute phase (in this study BALB/c), contrasting with the benign course of primary human infection. Surviving mice enter a chronic phase, and develop a characteristic inflammatory process suggested to have auto-immune component [2–4, 6–9]. In most mouse strains, parasite infection induces an extensive polyclonal lymphocyte activation, with a predominantly nonspecific immune response and increased levels of antibodies displaying NAb features [37]. As previously described, *Xid* mice control parasitemia, do not develop the characteristic wasting observed in the susceptible strains, mount limited polyclonal lymphocyte responses, and display reduced or absent tissue pathology on skeletal or cardiac muscles [11,12].

In our study, uninfected BA mice not only contained higher serum concentrations of IgM than *Xid*, but also displayed a relatively more reactive IgM repertoire than *Xid* animals, to both self (heart, liver) and non-self (*E. coli*, *T. cruzi*) antigens. Absolute serum IgM concentration and relative IgM reactivity to all examined extracts rose early after infection, coincidentally reaching highest levels in those typical BA mice that were individually more susceptible and died in the acute phase of infection. In contrast, all uninfected *Xid* mice presented an increased relative IgG reactivity to self tissues. This characteristic was particularly evident for autologous heart, where the reactivity pattern was dominated by the strong recognition of a specific protein band. Furthermore, on the basis of the IgG NAR it was possible to differentiate, within apparently identical susceptible isogenic mice, those that would resist infection and those that would not. In *Xid* and ‘atypical’ surviving BA mice, self-reactive, as well as some *E. coli*-reactive IgG were evidently decreased early after infection. Strikingly, a down-modulation of self-reactive IgG during infection of *Xid* mice occurred in parallel with, and apparently overproportionally contributed to, an absolute decrease of total serum IgG, a parameter that remained constant in ‘atypical’ BA mice. This contrasted with its increase observed in typical susceptible BA mice during the same period. Likewise, an overproportional and similarly extensive decrease in the dominant anti-heart IgG antibodies in *Xid* mice was observed following infection. Both of these phenomena were associated with a reciprocal behavior of IgM that apparently recognized the same antigen. This was consistent with

the total tissue-reactive IgM, which showed a most pronounced increase in most susceptible individuals. For both IgM and IgG, the statistical analysis of intrinsic repertoire structures by PCA confirmed these characteristics. In summary, after infection with *T. cruzi*, IgM and IgG mouse repertoire reactions were reciprocal between strains and also within individual BA mice: pre-existing and initially decreased natural IgG to specific and mainly self antigens was associated with a lower IgM reaction to all examined tissues and disease resistance. Conversely, high levels and rapid rise of reactive IgM was associated with little pre-existing natural IgG and no decrease, and more susceptibility to disease.

This observed progression of repertoire structure includes two new characteristics. First, both the differential antibody response and disease resistance of *Xid* appear to be associated with pre-existing NAR and thus not only to a reduced ability of Btk-mutant B cells to respond to T cell-independent activators [14–19]. These have been suggested to mediate the parasite-induced polyclonal activation [2, 4, 28], something that is equally reduced in *Xid* mice [11, 12]. Second, this is in agreement with our observation that several characteristics of the *Xid* response were to some extent shared by ‘atypical’ BA mice that were individually more resistant to *T. cruzi* infection than the great majority within the BA group. The combination of these two characteristics suggests that a mechanism of immunoregulation is involved and differentially developed in individual BA mice, but systematically reinforced in *Xid* mice. This implies that resistant *Xid* mice express a distinct set of IgG NAb. Hypothetically, these antibody specificities could regulate either the protective responses against parasite proteins, or a benign chronic disease with low levels of tissue pathology, as observed in *Xid* mice. Both assumptions may be valid, as we have recently found that sera from uninfected *Xid* mice contain antibodies that recognize (and neutralize?) a set of parasite molecules involved in the polyclonal activation that follows *T. cruzi* infection in susceptible BA mice [5]. Although simplistic, our preliminary results showed that the transfer of precipitated serum immunoglobulins from uninfected *Xid* mice to BA mice, and most particularly of protein A-Sepharose-purified IgG antibodies, leads to a control of acute levels of parasitemia after infective challenge and to a 50% decrease in mortality scores, as compared to saline-treated BA controls (not shown). These results are in agreement with our previous data [12, 13] showing that a combination of factors, and not exclusively antibodies, are necessary for the control of infection.

However, our present observations raise a number of further questions. NAb of the IgM, IgG and IgA isotypes are present in all normal individuals [38]. In contrast to puri-

fied IgG, however, the scoring of IgG reactivities in whole sera is usually poor, specifically inhibited by IgM NAb and/or other serum proteins [39, 40]. It follows that lower IgM concentration and/or a skewed IgM NAR structure in *Xid* mice could explain the apparent alterations of IgG NAR. The same line of reasoning could argue that an equivalent functional “release” of IgG NAR in *Xid* would favor a more efficient role in immune responses or in other regulatory mechanisms, particularly by limiting the disturbing effect of polyclonal lymphocyte activation. An additional hypothesis relating NAR and resistance to infection could invoke the established role of NAb in the selection of T cell repertoires [20, 21], which in turn could directly mediate resistance. Thus, we recently described that, in contrast to susceptible strains, the resistance of *Xid* mice is associated with an enhancement of Th-1 type activities resulting from B-1 cell deficiency, leading to IFN- $\gamma$ -mediated clearance of the parasites [12, 13]. In fact, this was the first demonstration that activation of B lymphocytes, most particularly B-1 cells, could determine the class of CD4 T cell responses. It is conceivable that the Btk mutation that has been shown to be directly responsible for the lack of B-1 cells, and deficits in IgM NAR and in conventional B cell signaling [14–21], could influence T cell repertoires, indirectly accounting for the generation of high levels of self-reactive, but non-pathological, IgG in naive *Xid* mice. Analogous alterations could occasionally also occur in congenic BA mice, due to other mechanisms that rely individually on different antigenic experience. A difference in the immune homeostasis, as outlined, could furthermore explain that the *Xid* mutation prevents the development of autoimmunity in lupus prone (NZB  $\times$  NZW) F1 mice [41]. Moreover, the differential resistance of *Xid* mice to both death in the acute phase and chronic myocarditis following *T. cruzi* infection is likely to be controlled by a co-operative mechanism, particularly because the present studies could not associate resistance to any particular characteristic of the specific antibody response to *T. cruzi* antigens.

B cells and immunoglobulins are evidently involved in the pathogenesis of some T cell-mediated autoimmune diseases, such as type I diabetes in NOD mice [42], and in the colitis of TCR $\alpha^{-/-}$  mice [43]. In general terms, “connected and multireactive” NAb have been suggested to participate in the maintenance of physiological autoreactivity [26, 27, 44], besides having a role in the early control of infectious agents [45]. On the other hand, such antibodies have also been considered as “precursors” of antibodies associated with pathological autoimmune reactions [46]. Either aspect of their physiopathology could finally be involved in the present observations, which encourage further investigation.

## 4 Materials and methods

### 4.1 Mice and infection

BALB/c were purchased from Charles Rivers (Saint-Aubins-Elbeuf, France) and BALB.*Xid* were maintained in our animal facilities; 8-week-old mice were used in all experiments. The CL strain of *T. cruzi* (clone F11F5) was maintained in our laboratory by sequential passage on C3H/HeJ mice. Experimental mice were inoculated i.p. with  $10^3$  trypanostigotes/mouse obtained from C3H/HeJ peripheral blood.

### 4.2 ELISA

Serum samples were collected by retro-orbital punctures on days 0, 3, 10, 20 and 35 after infection by retro-orbital plexus bleeding, and kept at  $-20^{\circ}\text{C}$  until use. ELISA were performed to determine total IgM and IgG concentrations, as described in detail elsewhere [35, 36]. Unlabeled purified IgM and IgG antibodies were used in serial dilution as standards. Sera were appropriately diluted in PBS-0.2% Tween 20 (PBS-T) so that all samples assayed finally contained  $10\ \mu\text{g/ml}$  IgM and  $100\ \mu\text{g/ml}$  IgG, respectively, when used in the immunoblot experiments.

### 4.3 Semiquantitative immunoblot analysis and image processing

Each extract, at a protein concentration of around  $600\ \mu\text{g/ml}$ , was applied to SDS-PAGE gels in a Mighty Small II SE 250 electrophoresis apparatus (Hoefer Scientific Instruments), and run at 45 mA until the front dye reached the bottom of the gel. After electrophoresis, the proteins were transferred to a nitrocellulose membrane (0.2 mm, Schleicher & Schuell) by semidry electrotransfer, for 1 h at  $0.8\ \text{mA/cm}^2$  using a semidry Electrobloater (Institut Pasteur, Paris). Following transfer, the membranes were blocked overnight with PBS-T at room temperature, incubated with the serum samples diluted in PBS-T for 4 h at room temperature using the Cassette Miniblot System (Immunetics Inc., Cambridge, MA), followed by repeated washes in PBS-T. Secondary alkaline phosphatase conjugated anti-mouse IgM or anti-mouse IgG antibodies (Southern Biotechnology) diluted in PBS-T were then added and incubated for 90 min at room temperature. After washing, immunoreactivities were revealed with nitroblue-tetrazolium/bromo-chloro-indolylphosphate (NBT/BCIP) substrate (Promega, Madison, WI) in appropriate buffer (100 mM Tris/HCl pH 9.5, 100 mM NaCl, 5 mM  $\text{MgCl}_2$ ). The reaction was stopped after 3–5 min by rinsing the membrane with distilled water. Quantitation of immunoreactivities was performed by densitometry in reflective mode, using a high resolution CCD camera system (Masterscan; Scanalytics, Billerica, MA). Total blotted proteins were then stained using colloidal gold (Protogold; Biocell, Cardiff, GB) and subjected to a second densitometric

analysis to score the protein profile. The scanned images were transformed into one-dimensional traces by the RFLPscan™ software (Scanalytics). Further data analysis was performed on a Power Macintosh 7500/100 computer (Apple Computer Inc.) using the software Igor (Wavemetrics, Lake Oswego, OR).

#### 4.4 Data sectioning

The two scans for immunoblot and protein staining were superimposed and profile migration irregularities corrected to allow the comparison of any serum immunoreactivity by specially developed macros for this software. Migration distances (x-axis) and light absorption (y-axis) were finally expressed as arbitrary units. Sera assayed on different membranes were normalized in relation to a standard (purified IgM or IgG), which was repeated in all membranes. The adjusted profiles were divided into sections for each respective extract (heart, liver, *T. cruzi* and *E. coli*). Section reactivities were then quantified as the average density within a respective section between two defined limits (total reactivity towards an extract was measured as the average density on the entire migration scale). Each serum can in this manner be represented as a vector with the section reactivities as co-ordinates, defined in a co-ordinate system (vector space) of a dimension equal to the number of section reactivities considered. This type of data cannot be illustrated in a simple manner. For the purpose of graphical representation, the numerical values obtained from the selected combinations of the immunoblots (number of sections/profile per extract) were submitted to PCA.

#### 4.5 Principal component analysis

PCA is a classical method of statistical analysis designed to describe multivariate and particularly correlated data with high dimensionality through projection on characteristic subspaces of lower dimensionality (*i.e.* a two-dimensional plot), simultaneously representing a maximal proportion of the information included in the data. Particularly, it uses the characteristic of eigenvectors of the data covariance matrix to fit the multidimensional data space. Experimental groups or other settings exert no influence upon this representation and, therefore, PCA provides a completely neutral method of representation. Resulting principal components, or PCA factors, are uncorrelated linear combinations of the underlying data (*i.e.* here the section reactivities) and ordered in terms of the degree of variance (*i.e.* relative information) they represent. The first principal component, or factor 1, represents the one-dimensional fitting vector, which contains the maximal possible proportion of the total information when data are projected on it. The 2nd principal component (factor 2) is the next optimal fitting vector, uncorrelated with the first factor, and so on. Special procedures for processing data and calculating PCA were developed for the 'Igor' software [29–34]. The theoretical aspects of the multivariate statistics are found elsewhere [47, 48].

#### 4.6 Hydrogen peroxide assay

The production of H<sub>2</sub>O<sub>2</sub> by peritoneal cells was measured by the horseradish peroxidase phenol red oxidation method, as described elsewhere [49]. Conversion of absorbance to nM H<sub>2</sub>O<sub>2</sub> was deducted from a standard curve for H<sub>2</sub>O<sub>2</sub>. All determinations were performed in quadruplicates.

**Acknowledgements:** We thank Drs. A. Ahouba, J. Demengeot and A. Waters, for their helpful discussions, and for reviewing this manuscript. This work was supported by Institut Pasteur (France), CNRS URA 1960 (France) and ANRS (France). Corresponding support was given to: R.V. (CNPq no. 20.050993 and UFF, Brazil), E.S.L. (CNPq 201412/92-6, Brazil), B.R.S.M. (CONACyT no. 94587, México), C.F. (DAAD, Germany) and A.C.S. (JNIC-T-CNRS, BD529/92, France/Portugal).

#### References

- 1 **Ribeiro-dos-Santos, R. and Rossi, M. A.,** Immunopatologia. In **Cançado, R. and Chuster, M.** (Eds.) *Cardiopatia Chagastica*, chapter 2. Fundação Carlos Chagas, Belo Horizonte 1985, p 10.
- 2 **Minoprio, P., Itohara, S., Heusser, C., Tonegawa, S. and Coutinho, A.,** Immunobiology of murine *T. cruzi* infection: the predominance of parasite-nonspecific responses and the activation of TCRI T cells. *Immunol. Rev.* 1989. **112**: 183–207.
- 3 **Tarleton, R. L. and Kuhn, R. E.,** Measurement of parasite-specific immune responses in vitro: evidence for suppression of the antibody response to *Trypanosoma cruzi*. *Eur. J. Immunol.* 1985. **15**: 845–850.
- 4 **Minoprio, P., Eisen, H., Forni, L., d'Imperio-Lima, M. R., Joskowicz, M. and Coutinho, A.,** Polyclonal lymphocyte responses to murine *Trypanosoma cruzi* infection. I. Quantitation of both T and B cell responses. *Scand. J. Immunol.* 1986. **24**: 661–668.
- 5 **Reina-San-Martin, B., Degraeve, W., Rougeot, C., Cosson, A., Chamond, N., Cordeiro-da-Silva, A., Arala-Chaves, M. and Minoprio, P.,** A B cell mitogen from a pathogenic trypanosome is a eukaryotic proline racemase. *Nat. Med.* 2000. **6**: 890–897.
- 6 **Kierszenbaum, F.,** Chagas' disease and the autoimmune hypothesis. *Clin. Microbiol. Rev.* 1999. **12**: 210–223.
- 7 **Zhang, L. and Tarleton, R.,** Parasite persistence correlate with disease severity and localization in chronic Chagas' disease. *J. Infect. Dis.* 1999. **180**: 480–486.
- 8 **Eisen, H. and Kahn, S.,** Mimicry in *Trypanosoma cruzi*: fantasy and reality. *Curr. Opin. Immunol.* 1991. **3**: 507–510.
- 9 **Dziarski, R.,** Autoimmunity: polyclonal activation or antigen induction? *Immunol. Today* 1988. **9**: 340–342.
- 10 **Coutinho, A., Forni, L., Holmberg, D., Ivars, F. and Vaz, N.,** From an antigen-centered, clonal perspective of autonomous activity in a self-referencial immune system. *Immunol. Rev.* 1984. **79**: 151–168.
- 11 **Minoprio, P., Coutinho, A., Spinella, S. and Hontebeyrie-Joskowicz, M.,** Xid immunodeficiency imparts increased parasite clearance and resistance to pathology in experimental Chagas' disease. *Int. Immunol.* 1991. **3**: 427–433.
- 12 **Minoprio, P., Cury-EI-Cheikh, M., Murphy, E., Hontebeyrie-Joskowicz, M., Coffman, R., Coutinho, A. and O'Garra, A.,**

- Xid-associated resistance to experimental Chagas' disease is IFN- $\gamma$ -dependent. *J. Immunol.* 1993. **151**: 4200–4208.
- 13 **Cordeiro-da-Silva, A., Lima, E. C. S., Vicentelli, M.-H. and Minoprio, P.**, V $\beta$ 6-bearing cells are involved in resistance to *Trypanosoma cruzi* infection in XID mice. *Int. Immunol.* 1996. **8**: 1213–1219.
  - 14 **Khan, W., Alt, F., Gerstein, R., Malyin, B., Rathbun, I., Davidson, L., Muller, S., Kantor, A., Herzenberg, L. A., Rosen, F. and Sideras, P.**, Defective B cell development and function in Btk-deficient mice. *Immunity* 1995. **3**: 283–289.
  - 15 **Scher, I., Ahmed, A., Strong, D., Steinberg, A. and Paul, W.**, X-linked B lymphocyte immune defect in CBA/N mice. *J. Exp. Med.* 1975. **141**: 788–803.
  - 16 **Wicker, L. and Scher, F.**, X-linked immunodeficiency (xid) of CBA/N mice. *Curr. Top. Microbiol. Immunol.* 1986. **124**: 87–99.
  - 17 **Scher, I.**, The CBA/N mouse strain: an experimental model illustrating the influence of the X-chromosome on immunity. *Adv. Immunol.* 1982. **33**: 1–71.
  - 18 **Hayakawa, K., Hardy, R. R., Parks, D. R. and Herzenberg, L. A.**, The Ly-1 B cell population in normal, immunodeficient and autoimmune mice. *J. Exp. Med.* 1983. **157**: 202–218.
  - 19 **Santos-Argumedo, L., Lund, F. E., Heath, A. W., Solvason, N., Wu, W. W., Grimaldi, J. C., Parkhouse, R. M. E. and Howard, M.**, CD38 unresponsiveness of xid B cells implicates Bruton's tyrosine (btk) as a regulator of CD38 induced signal transduction. *Int. Immunol.* 1995. **7**: 163–170.
  - 20 **Herzenberg, L. A., Stall, A. M., Lalor, P. A., Sidman, C., Moore, W. A., Parks, D. R. and Herzenberg, L. A.**, The Ly-1 B cell lineage. *Immunol. Rev.* 1986. **93**: 81–102.
  - 21 **Marcos, M. A. R., Toribio, M.-L., De-La-Hera, A., Márquez, C., Gaspar, M.-L. and Martínez-A., C.**, Mutual cell interaction and the selection of immune repertoires. *Immunol. Today* 1988. **9**: 204–207.
  - 22 **Minoprio, P., Bandeira, A., Pereira, P., Mota-Santos, T. A. and Coutinho, A.**, Preferential expansion of Ly1-B and CD4<sup>+</sup> CD8<sup>+</sup> T cells in the polyclonal lymphocyte responses to murine *Trypanosoma cruzi* infection. *Int. Immunol.* 1989. **1**: 176–184.
  - 23 **Hitoshi, Y., Okada, Y., Sonoda, E., Tominaga, A., Makino, M., Suzuki, K., Kinoshita, J., Komuro, K., Mizuochi, T. and Takatsu, K.**, Delayed progression of a murine retrovirus-induced acquired immunodeficiency syndrome in X-linked immunodeficient mice. *J. Exp. Med.* 1993. **177**: 621–626.
  - 24 **Hoerauf, A., Solbach, W., Lohoff, M. and Rölinghoff, M.**, The Xid defect determines an improved clinical course of murine leishmaniasis in susceptible mice. *Int. Immunol.* 1994. **6**: 1117–1124.
  - 25 **Zhao, Y.-X., Abdelnour, A., Holmdahl, R. and Tarkowski, A.**, Mice with the Xid B cell defect are less susceptible to developing *Staphylococcus aureus*-induced arthritis. *J. Immunol.* 1995. **155**: 2067–2076.
  - 26 **Boyden, S.**, Natural antibodies and the immune response. *Adv. Immunol.* 1966. **5**: 1–28.
  - 27 **Michel, C., Gonzales, R., Bonjour, E. and Avrameas, S.**, A current increasing of natural antibodies and enhancement of resistance of furunculosis in rainbow trout. *Ann. Rech. Vet.* 1990. **21**: 211–218.
  - 28 **d'Imperio-Lima, M. R., Eisen, H., Minoprio, P., Jaskowicz, M. and Coutinho, A.**, Persistence of polyclonal B cell activation with undetectable parasitemia in late stages of experimental Chagas' disease. *J. Immunol.* 1986. **137**: 353–356.
  - 29 **Haury, M., Gradien, A., Sunblad, A., Coutinho, A. and Nobrega, A.**, Global analysis of antibody repertoires. I. An immunoblot method for the quantitative screening of a large number of reactivities. *Scand. J. Immunol.* 1994. **39**: 79–87.
  - 30 **Nobrega, A., Haury, M., Gradien, A., Malanchère, E., Sundblad, A. and Coutinho, A.**, Global analysis of antibody repertoires. II. Evidence for specificity, self-selection and the immunological "homunculus" of antibodies in normal serum. *Eur. J. Immunol.* 1993. **23**: 2851–2859.
  - 31 **Sundblad, A., Marcos, M. A., Malanchère, E., Castro, A., Haury, M., Huetz, F., Nobrega, A., Freitas, A. and Coutinho, A.**, Observations on the mode of action of normal immunoglobulin at high doses. *Immunol. Rev.* 1994. **139**: 125–158.
  - 32 **Mouthon, L., Nobrega, A., Nicolas, N., Kaveri, S. V., Barreau, C., Coutinho, A. and Kazatchkine, M. D.**, Invariance and restriction toward a limited set of self-antigens characterize neonatal IgM antibody repertoires and prevail in autoreactive repertoires of healthy adults. *Proc. Natl. Acad. Sci. USA* 1995. **92**: 3839–3843.
  - 33 **Fesel, C. and Coutinho, A.**, Dynamics of serum IgM autoreactive repertoires following immunization: strain specificity, inheritance and association with autoimmune disease susceptibility. *Eur. J. Immunol.* 1998. **28**: 3616–3629.
  - 34 **Ferreira, C., Mouthon, L., Nobrega, A., Haury, M., Kazatchkine, M., Ferreira, E., Padua, F., Coutinho, A. and Sundblad, A.**, Instability of natural antibody repertoires in systemic lupus erythematosus patients, revealed by multiparametric analysis of serum antibody reactivities. *Scand. J. Immunol.* 1997. **45**: 331–341.
  - 35 **Holmberg, D., Forsgren, S., Ivars, F. and Coutinho, A.**, Reactions among IgM antibodies derived from normal, neonatal mice. *Eur. J. Immunol.* 1984. **14**: 435–441.
  - 36 **Malanchère, E., Marcos, M. A. R., Nobrega, A. and Coutinho, A.**, Studies on the T cell dependence of natural IgM and IgG antibody repertoires in adult mice. *Eur. J. Immunol.* 1995. **25**: 1358–1365.
  - 37 **Minoprio, P., Burlen, O., Pereira, P., Guilbert, B., Andrade, L., Hontebeyrie-Joskowicz, M. and Coutinho, A.**, Most B cells in acute *Trypanosoma cruzi* infection lacks parasite specificity. *Scand. J. Immunol.* 1988. **28**: 553–561.
  - 38 **Avrameas, S.**, Natural antibodies: from "horror autotoxicus" to "gnothi seauton". *Immunol. Today* 1991. **12**: 154.
  - 39 **Hurez, V., Kaveri, S. and Kazatchkine, M.**, Expression and control of the natural autoreactive IgG repertoire in normal human serum. *Eur. J. Immunol.* 1993. **23**: 783–789.
  - 40 **Saenko, V. A., Kabakov, A. E. and Poverenny, A. M.**, Hidden high-avidity anti-DNA antibodies occur in normal human gammablobulin preparations. *Immunol. Lett.* 1992. **34**: 1–5.
  - 41 **Steinberg, B. J., Smathers, P. A., Frederiksen, K. and Steinberg, A. D.**, Ability of the Xid gene to prevent autoimmunity in (NZB xNZB)F1 mice during the course of their natural history, after polyclonal stimulation, or following immunization with DNA. *J. Clin. Invest.* 1982. **70**: 587–597.
  - 42 **Akashi, T., Nagafuchi, S., Anzai, K., Kondo, S., Kitamura, D., Ono, S., Kikuchi, M., Niho, Y. and Watanabe, T.**, Direct evidence for the contribution of B cells to the progression of insulinitis and the development of diabetes in non-obese mice. *Int. Immunol.* 1997. **9**: 1159–1164.
  - 43 **Mizoguchi, A., Mizoguchi, A., Smith, R. N., Preffer, F. I. and Bhan, A. K.**, Suppressive role of B cells in chronic colitis of T cell receptor alpha mutant mice. *J. Exp. Med.* 1997. **186**: 1749–1756.
  - 44 **Coutinho, A., Kazatchkine, M. and Avrameas, S.**, Natural auto-antibodies. *Curr. Opin. Immunol.* 1995. **7**: 812–818.

- 45 **Navin, T., Krug, E. and Pearson, R.**, Effect of immunoglobulin M from normal human serum on *Leishmania donovani* promastigote agglutination, complement-mediated killing and phagocytosis by human monocytes. *Infect. Immun.* 1989. **57**: 1343–1346.
- 46 **Mendlovic, S., Broke, S., Shoenfeld, Y., Ben-Bassat, M., Meshorer, A., Bakimer, R. and Mozes, E.**, Induction of a systemic lupus-erythematosus-like disease in mice by a common human anti-DNA idiotype. *Proc. Natl. Acad. Sci. USA* 1988. **82**: 2260–2264.
- 47 **Jobson, J.**, *Applied multivariate data analysis: categorical and multivariate methods*. Springer-Verlag, New York 1992.
- 48 **Lebart, L., Morineau, A. and Fenelon, J.**, *Traitement des données statistiques*. Dunod, Paris 1982.
- 49 **Pick, E. and Mizel, D.**, Rapid microassays for the measurement of superoxide and hydrogen peroxide production by macrophages in culture using an automatic enzyme immunoassay reader. *J. Immunol. Methods* 1981. **46**: 211–226.

---

**Correspondence:** Paola Minoprio, Département d'Immunologie, Institut Pasteur, 25 rue du Dr. Roux, 75724 Paris CEDEX 15, France

Fax: +33-1-45688615

e-mail: pmm@pasteur.fr

Present addresses: R. Vasconcelos, Universidade Federal Fluminense, Niteroi, Brasil; A. Cordeiro-da-Silva, Faculdade de Farmacia, Universidade do Porto, Porto, Portugal